PHYSICOCHEMICAL PROPERTIES AND SOLUBILITY OF PIPERAZINE ACTIVATED AQUEOUS SOLUTION OF ß-ALANINE AS A SOLVENT FOR CO_2 CAPTURE

By

NOR AISYAH BINTI AZMI
15088

Dissertation submitted in partial fulfilment of the requirements for the
Bachelor of Engineering (Hons)
(Chemical)

MAY 2014

Universiti Teknologi PETRONAS
Bandar Seri Iskandar
31750 Tronoh
Perak Darul Ridzuan

CERTIFICATION OF APPROVAL

PHYSICOCHEMICAL PROPERTIES AND SOLUBILITY OF PIPERAZINE ACTIVATED AQUEOUS SOLUTION OF ß-ALANINE AS A SOLVENT FOR CO_2 CAPTURE

by

NOR AISYAH BINTI AZMI

15088

A project dissertation submitted to the
Chemical Engineering Programme
Universiti Teknologi PETRONAS
in partial fulfilment of the requirement for the

BACHELOR OF ENGINEERING (Hons)
(CHEMICAL)

Approved by,

_____

(Dr. Ghulam Murshid)

UNIVERSITI TEKNOLOGI PETRONAS
TRONOH, PERAK
MALAYSIA

MAY 2014

CERTIFICATION OF ORIGINALITY

This is to certify that I am responsible for the work submitted in this project, that the original work is my own except as specified in the references and acknowledgements, and that the original work contained herein have not been undertaken or done by unspecified sources or persons.

_____

(Nor Aisyah Binti Azmi)

ABSTRACT

Carbon dioxide is one of the major greenhouse gas (GHG) contributors. It is an obligation for the industry to reduce the amount of carbon dioxide emission to the atmosphere. Tremendous research and studies are being done in order to develop the most plausible absorber for carbon dioxide removal. Amino acids are being looked into by the industry as a potential solvent for absorption of carbon dioxide to replace alkanolamines due to its ability to resist oxidative degradation, low volatility due to its ionic structure and higher surface tension. In addition, the introduction of promoter-like piperazine to amino acid helps to further enhance the solubility effect by acting as catalyst to speed up absorption process. In this work, the effect of piperazine activated aqueous solutions of B-alanine on physicochemical properties and solubility of CO_2 is studied for various correlations. The properties are measured over a wide range of temperature from (30-60) ^{0}C. The effect of activator piperazine on the CO_2 loading performance of selected amino acid under high-pressure conditions (1bar to 10bar) at temperature range of (30-60) ^{0}C was studied. From the observations, the density and surface tension of piperazine activated aqueous solutions of B-alanine decreases when the piperazine concentration increases. It was noticed that the density and surface tension decreases with increasing piperazine concentration in the blends. Density, viscosity and refractive index decrease with increasing temperature. Surface tension of piperazine activated aqueous solutions of B-alanine increases with increasing temperature. The value measured for physicochemical properties were correlated as a function of temperature using least-squares method and the correlation parameters are reported together with it respective standard deviation. Solubility of CO_2 increases with decreasing temperature and increasing pressure. Quadratic representation of solubility using Response Surface Methodology (RSM) is generated and from the findings, the most important parameter to optimize solubility is system pressure. Addition of piperazine to amino acids solutions can increase the solubility effect of the solvent.

TABLE OF CONTENTS

LIST OF TABLES

LIST OF FIGURES

ABBREVIATION

BALA	B-alanine
BASF	Baden Aniline and Soda Factory
DEA	Diethanolamine
DIPA	Di-isopropanolamine
GHG	Greenhouse gas
MDEA	Monodiethanolamine
MEA	Monoethanolamine
PZ	Piperazine
RSM	Response Surface Methodology

CHAPTER 1: INTRODUCTION

1.1 Background

Global warming and climate change are resulted from greenhouse gases that are emitted to the atmosphere. Carbon dioxide is believed to be the major contributor for this problem. Most carbon dioxide comes from energy generation from the combustion of fossil fuels. If combined with water, it has the ability to corrode and destroy pipelines. Thus, technologies on the carbon dioxide capture are thoroughly being looked into. Absorption, adsorption, membrane and cryogenic process are the technologies that are commonly used in the industry (Rao & Rubin, 2002). Optimizations of absorption by various type chemical solvents are continuously being improved and developed by researchers to get high reactivity, low solvent cost, low absorption of hydrocarbon, and low oxidative degradation. Previously, alkanolamines like monoethanolamine (MEA) and diethanolamine (DEA) are commonly used as a CO_2 absorber due to fast reaction kinetics and low solvent cost. However, disadvantages of MEA are it induced oxygen degradation, metal corrosion, and high regeneration energy (Sakwattanapong, Aroonwilas, & Veawab, 2005; Soosaiprakasam & Veawab, 2008; Supap, Idem, Tontiwachwuthikul, & Saiwan, 2009). Amino acids are identical to alkanolamines because of the presence of similar functional group in the molecule. Amino acids are considered the alternative of alkanolamines because of its ability to resist oxidative degradation, low volatility due to its ionic structure and higher surface tension compared to alkanolamines (Hook, 1997; Song et al., 2012). Modification of amino acid based solvent have the ability to produce more sophisticated and enhanced characteristic towards CO_2 absorption by blending promoters and other compounds (Shaikh, Shariff, Bustam, & Murshid, 2013). In this project, non-sterically hindered linear amino acid B-Alanine (BALA) will be blend with promoter piperazine. Reason being, B-Alanine(BALA) formed more (bi)carbonate compared to MEA and it will directly enhance the CO_2 absorption (Mergler, Gurp, Brasser, Koning, & Goetheer, 2011). Meanwhile, piperazine(PZ) had been proven as effective activator for alkanolamines due to the rapid formation of carbamate with CO_2. Piperazine activated MDEA technology is already patterned by

BASF (Bougie & Iliuta, 2011). The aqueous solution of BALA and PZ will induce high formation of bicarbamate. Thermodynamics properties of BALA and PZ blends such as density, viscosity, surface tension and refractive index of this solution must be known to understand the intermolecular interactions and to design the acid gas absorption system (Derks, Hogendoorn, & Versteeg, 2005).Thus in this research paper, the physicochemical properties and CO_2 solubility of aqueous solution B-Alanine and piperazine (BALA+PZ) are measure over a wide range of temperature at different BALA to PZ ratio will be reported.

1.2 Problem Statement

Carbon dioxide is the world major greenhouse gas (GHG) contributor. As the world is going green, it is an obligation for the industry to reduce the amount of carbon dioxide emission to the atmosphere. Tremendous researches and studies are being done in order to develop the most plausible absorber for carbon dioxide. Previously, alkanolamines like monoethanolamine (MEA) and diethanolamine (DEA) are commonly used as a CO_2 absorber due to fast reaction kinetics and low solvent cost. However, drawbacks of MEA are it induced oxygen degradation, metal corrosion, and high regeneration energy. Alternative of alkanolamine are amino acid, both exhibit almost similar functional group, C-OH and C-OOH respectively. It is believed that amino acid has the ability to resist oxidative degradation and low volatility. This opens new opportunity for researchers to come out with new blends with promoter-like piperazine with amino acid. To ensure the new blend is fit for industrial practice, it is crucial to study the physical properties and solubility of CO_2 of the respective blends at various ratio and temperature. This project will study the effect of promoter piperazine (PZ) on physicochemical properties and solubility of carbon dioxide (CO_2) in B-Alanine (BALA) at various concentration, pressure and temperature.

1.3 Objectives

The main objectives of project are as follows:

1) To determine the physicochemical properties of piperazine activated aqueous solution of B-Alanine over a wide range of temperature for various concentrations of B-Alanine and piperazine.
2) To determine the effect of pressure, temperature and concentration of piperazine activated aqueous solution of B-Alanine on CO_2 solubility.

1.4 Scope of Study

This experiment will use piperazine and B-alanine blends as CO_2 absorber. The manipulated variable will be the ratio of PZ to BALA and temperature of the blends. For each of the blends, two responding variables will be determined. The blending ratio of aqueous BALA/PZ will be varied from 10% to 30% mass fractions. The temperature range of the experiment is 30^oC to 60^oC. The first responding variable is the physicochemical properties of the blends including the density, viscosity, surface tension and refractive index. The next variable that will be the measured is CO_2 solubility in the respective blends. The behavior and trend of piperazine activated aqueous solution of B-alanine over wide range of temperature and pressure will be determined by using high-pressure solubility cell.

CHAPTER 2: LITERATURE REVIEW AND THEORY

2.1 Literature Review and Theory

Combustion of fuels had increased the concentration of CO_2 in the atmosphere. High CO_2 concentration will lead to climate change and global warming. This had raised the world awareness to improve the efficiency of CO_2 capture technology. Absorption, adsorption, membrane and cryogenic process are among the technologies that are commonly used in the industry. Absorption is one of a mature and promising method to separate CO_2 from gas mixtures(Rao & Rubin, 2002).

Absorption is a mass transfer process between gas and liquid whereby gas is absorbed into liquid. Gas absorbed and liquid is referred to absorbate and absorbent respectively. Generally, ideal absorbent should have a high solubility for the solute, low volatility, stable, non-corrosive, low viscosity, low foaming, nontoxic and nonflammable. The most commonly used absorbent are water, hydrocarbon oil and aqueous solution of acid and bases(Geankoplis, 2003). **Figure 1** shows a separation column for absorption. Liquid inlet refers to the absorbent and gas inlet refers to CO_2 gas. Both liquid and gas will contact in countercurrent manner. Unwanted gas will be captured in the liquid and leaves at the bottom of the column.

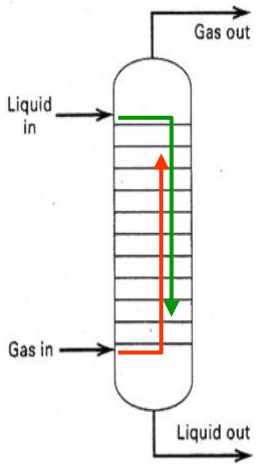

Figure 1: Absorption column

The common chemical solvents used as absorbent are alkanolamines like monoethanolamine (MEA), di-ethhanolamine (DEA), and di-isopropanolamine (DIPA). Alkanolamines are used as CO_2 absorber due to fast reaction kinetics and low solvent cost. Disadvantages of MEA are it induced oxygen degradation and will induced metal corrosion in pipelines, and high regeneration energy (Sakwattanapong et al., 2005; Soosaiprakasam & Veawab, 2008; Supap et al., 2009).

Thus, researchers come out with amino acid that exhibits almost similar functional group to alkanolamines(Song et al., 2012). Amino acid had become the alternatives of alkanolamines for CO_2 capture due to low volatility and resistance to oxidative degradation. Modification of amino acid with other compounds imparts more novel characteristics in the solvent and directly improves the absorption properties of the solvent (Shaikh et al., 2013).

Amino acids are further categorized into four groups, linear amino acid, sterically hindered amino acids, cyclic amino acids and poly amino acids. Based on the molecular structure, the CO_2 absorption and desorption of amines can be predicted. The closer the carboxylic and amino group, the steric repulsion are expected to be stronger(Song et al., 2012). B-alanine structure **(Figure 2)** has faster initial absorption rate compared to Glycine **(Figure 3)** due to the longer distance between the amino to carboxylic groups.

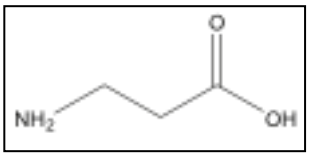

Figure 2: B-alanine structure

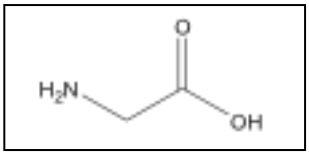

Figure 3: Glycine Structure

The overall reaction of CO_2 removal in aqueous amino acid can be represented as **Equation 1** and **2**.

$$CO_2 + H_2O \leftrightarrow HCO_3^- + H^+ \quad \text{(Equation 1)}$$

$$CO_2 + BALA \leftrightarrow BALACOO^- + H^+ \quad \text{(Equation 2)}$$

Promoter or activators are added to aqueous solution to enhance the reaction rate. Promoter can be termed as homogenous catalysis. General mechanism for this reaction by **Equation 3** and **4** (Astarita, Savage, & Longo, 1981).

$$CO_2 + \text{promoter} \leftrightarrow \text{intermediate} \quad \text{(Equation 3)}$$

$$\text{Intermediate} + OH^- \leftrightarrow \text{promoter} + HCO_3^- \quad \text{(Equation 4)}$$

Piperazine(PZ) had been proven as effective activator for alkanolamines due to the rapid formation of carbamate with CO_2. Piperazine activated MDEA technology is already patterned by BASF (Bougie & Iliuta, 2011). Piperazine **(Figure 4)** has di-amine that can react with CO_2. **Equation 5** and **6** shows the mechanism of piperazine (Bishnoi & Rochelle, 2000) .

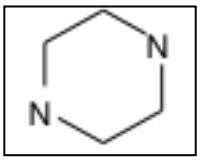

Figure 4: Piperazine structure

$$PZ + CO_2 \leftrightarrow PZCOO \quad \text{(Equation 5)}$$

$$PZCOO^- + OH^- \leftrightarrow PZ + HCO_3^- \quad \text{(Equation 6)}$$

Song et al.; (2012) added a small amount of piperazine to alanine, serine, α-aminobutyric acid. The result of piperazine addition had increased the net cyclic capacity to 25%. This result shows that amino acid can be energy-efficient and have a huge potential to be utilized as CO_2 absorbing liquid.

A research was done to study the physicochemical properties of amino acid namely sodium glycinate and piperazine blends for CO_2 capture. This experiment measures the density, viscosity and refractive index of the blends. With increasing temperature, the density, viscosity and refractive index of glycinate and piperzine will decrease(Shaikh et al., 2013). Hydrodynamics and mass transfer rates in absorption is highly affected by liquid phase viscosity and surface tension(Muhammad, Mutalib, Wilfred, Murugesan, & Shafeeq, 2008).

Natural gas sweetening and pre-combustion process demand high pressure CO_2 removal. The capacity for absorption can be studied in terms of CO_2 solubility(Shariff, Murshid, Lau, Bustam, & Ahamd, 2011). A study on solubility in aqueous solution of 2-amino-2-methyl-1-propanol (AMP) at high pressure by Shariff et al, (2011) on various range of pressure of industrial interest shows that solubility increases with increasing pressure and decreases with increasing temperature.

The aqueous solution of BALA and PZ will induce high formation of bicarbonate (Mergler et al., 2011).Thermodynamics properties of BALA+PZ blends such as density, viscosity, surface tension and refractive index of this solution must be known to understand the intermolecular interactions an to design the acid gas absorption system (Derks et al., 2005).

Thus in this research paper, the physicochemical properties and CO_2 solubility of aqueous solution B-alanine and piperazine (BALA+PZ) are measure over a wide range of temperature at different BALA/PZ ratio will be reported.

CHAPTER 3: METHODOLOGY/ PROJECT WORK

In this research activity, the methodology can be divided into two parts. The first part is on physicochemical properties of B-alanine and piperazine blends over temperature range (30-60) ^{0}C. Meanwhile on the second part, the research will be focused on solubility of B-alanine and piperazine blends on CO_2.

There will be three B-alanine and piperazine blends used in this research. The purpose of this experiment is to determine the novelty of B-alanine and piperazine blends as a medium of CO_2 capture and is fit to be used by the industry.

3.1 Project Methodology

The main flow of project is as follows:

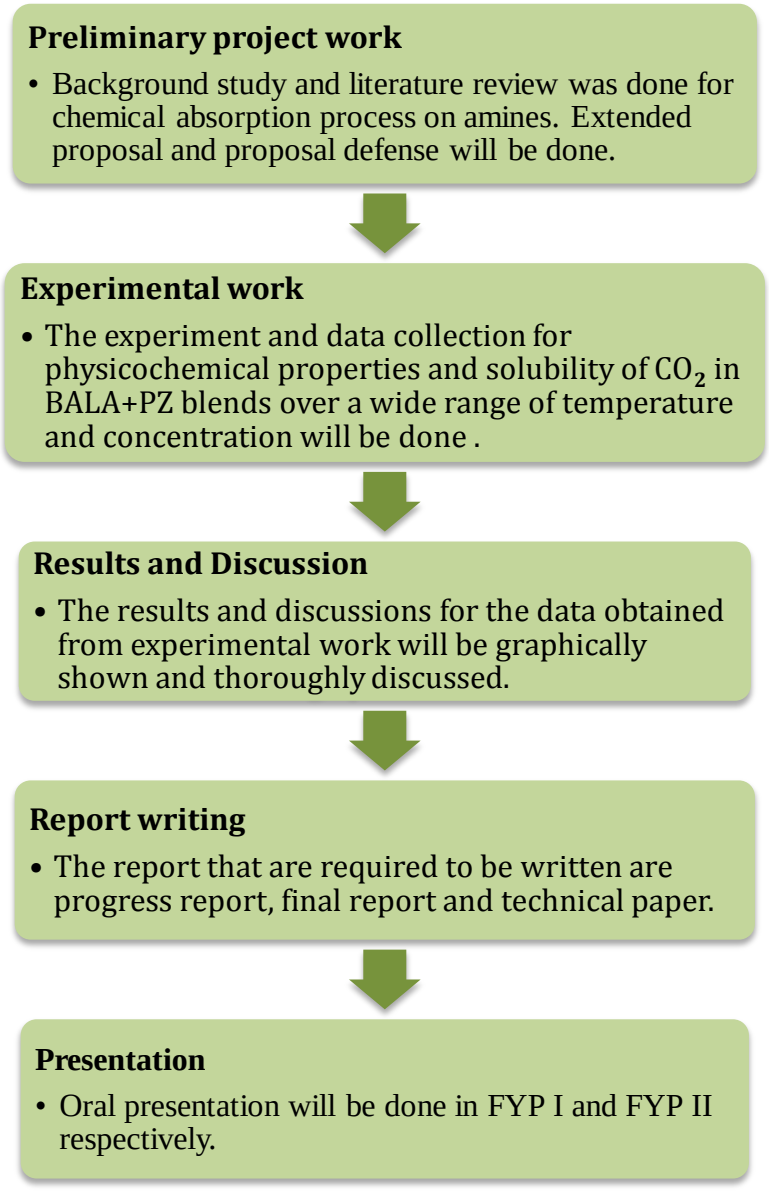

3.2 Material and Equipment

The main reagent for this project is linear amino acid, B-alanine (≥ 99% pure) and promoter piperazine (≥ 99% pure) were obtained from Merck Sdn. Bhd, Malaysia. Different blends of (BALA+PZ) will be prepared using double-distilled water. The blending ratio of aqueous BALA/PZ will be approximately 10% to 30% of mass fractions and prepared gravimetrically by using n analytical balance (Mettler Toledo AS120S) with the accuracy of ± 0.0001 g. Carbon dioxide with 99.99% purity was obtained from Malaysia Oxygen Berhad (MOX Gasses).

Equipment for physicochemical properties experiment:

Table 1: Physicochemical properties experimental equipment and measurement

Measurement	Equipment	Accuracy
Density	Digital Anton Par density meter (DMA-4500M)	± 0.0003 $g \cdot cm^{-3}$
Viscosity	Digital Anton Par microviscometer (Lovis-2000M)	± 0.002 mPa·s
Surface Tension	Pendent drop method, VINCI technologies (IFT 700)	± 0.03 $mN \cdot m^{-1}$
Refractive Index	Digital Anton Par refractometer (Abbemet)	± 0.005K

Equipment for CO_2 solubility:

Table 2: CO_2 solubility experimental equipment and measurement

Measurement	Equipment	Accuracy
CO_2 Solubility	High Pressure Solubility Cell (SOLTEQ BP-22)	± 0.0003 $g \cdot cm^{-3}$
System Pressure	Digital Pressure Indicator (Druck DPI 150)	± 1 bar
System Temperature	Thermostat water bath Julabo	± 0.1 °C
Temperature of mixing vessel and solubility cell	Digital Thermometer (YOKOGAVA 7653)	± 0.01 °C

3.3 Project Activities

3.3.1 Experimental Methodology

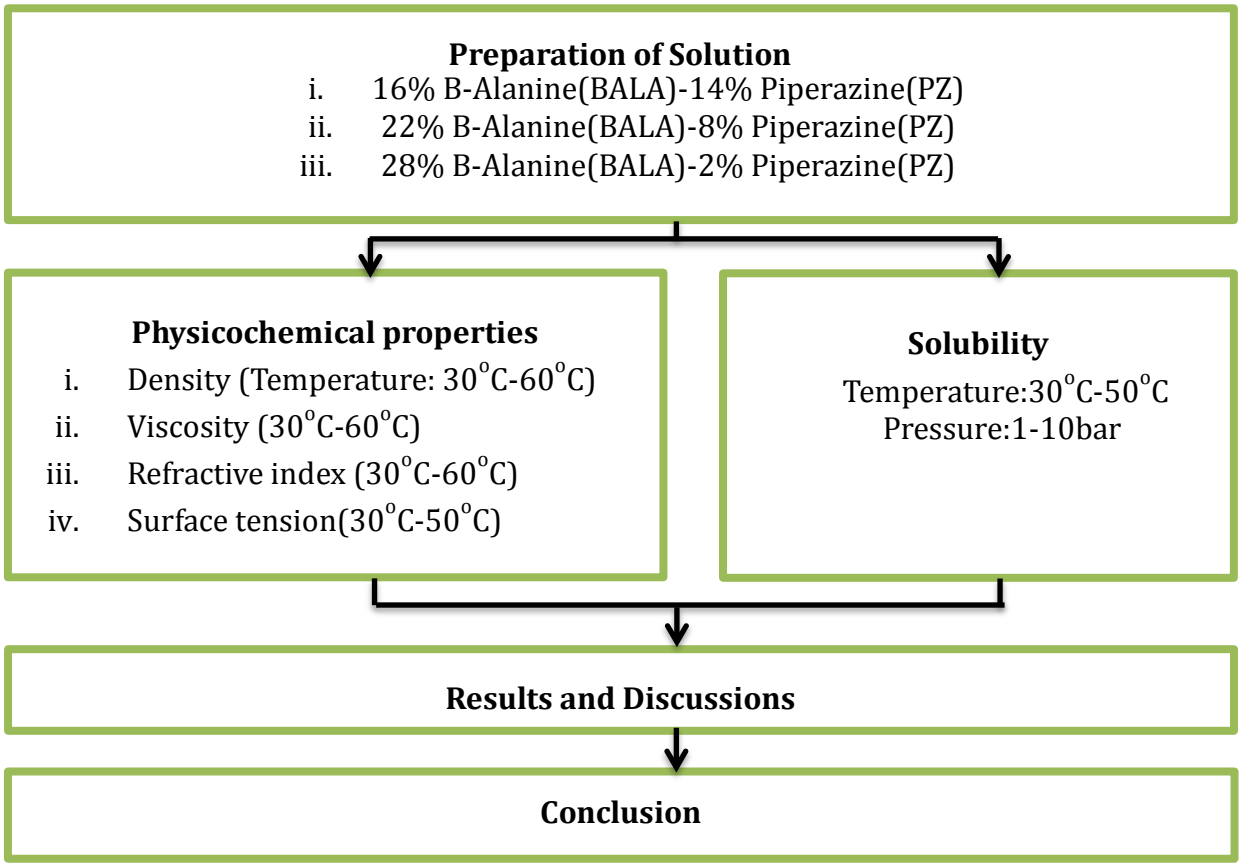

3.3.2 Physicochemical Properties Experiment

Density Measurement

Density of different blends of (PZ+BALA) are measured using digital Anton Par density meter (DMA-4500M).The density and temperature accuracy of the equipment is ± 0.00003g.cm^{-3}and ±0.01K respectively. The equipment was calibrated by using standard water Millipore quality repeatedly after completing each measurement to minimize the error. Data averages of three measurements were reported.

Viscosity Measurement

Viscosities of piperazine activated aqueous solution of B-alanine are measured using digital rolling ball Anton Par micro viscometer (Lovis-2000M).The equipment accuracy is up to 0.5%.The estimated viscosity and temperature uncertainties were

$\pm 7.10^{-3}$mPa.s and ± 0.02K respectively. The equipment was calibrated repeatedly by using standard water Millipore quality after completing each measurement. Samples were kept inside viscometer until the set temperature reach equilibrium conditions before measurement are taken. Triplicate readings were taken and reported as average in the data.

Refractive Index Measurement

Refractive indices of piperazine activated aqueous solution of B-alanine were measured using digital Anton Par refractometer (Abbemet) under a wide range of temperature with ±0.05K accuracy. Prism face must be cleaned with acetone and dried to avoid discrepancy by minutes sediments before placing the sample into sample holder. Measurements were taken after placing the sample into sample holder and set the equipment at the desired temperature. The equipment is calibrated by using standard water Millipore quality after completing each measurement repeatedly after completing each measurement to reduce the error. The averages of three readings were reported with ±0.00005nD accuracy.

Surface Tension Measurement

Surface tensions of piperazine activated aqueous solution of B-alanine are measured by using IFT 700 (VINCI Technologies) with $\pm 0.03 mN.m^{-1}$ accuracy. Pendent drop method was used to measure the surface tension of the solvent where the shape and contact angle properties of a drop created inside a thermostatic chamber was captured and recorded. The averages of five measurements were reported with experimental and temperature uncertainties of 0.05 $mN.m^{-1}$ and 0.2K respectively.

3.3.3 Solubility Measurement

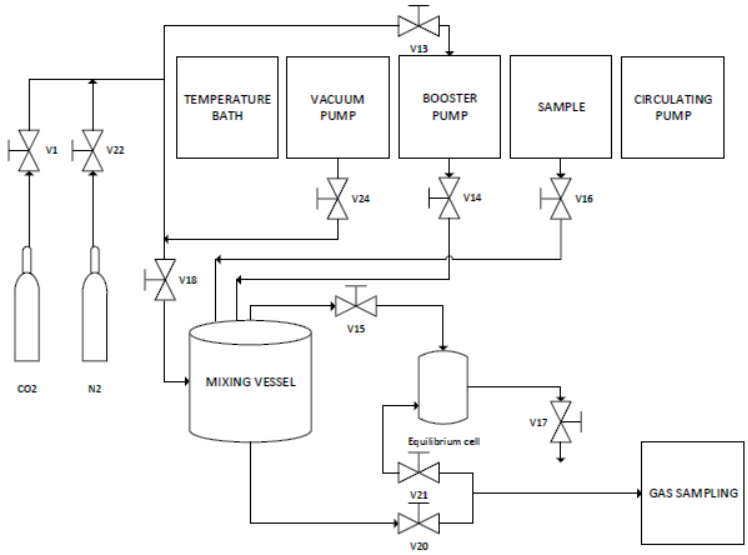

Figure 5: Schematic diagram of high pressure solubility experiment

Solubility measurements are conducted in high-pressure solubility cell (SOLTEQ BP-22). The schematic diagram is shown in **Figure 5**. The main components and function of high pressure solubility cell are listed in **Table 3**.

Table 3: Components and functions of high pressure solubility cell equipment

Component	Function
Mixing Vessel (B1)	For initial charging and pressurization of gas mixtures.
Equilibrium Cell (B2)	For dissolving gas mixture into liquid
Gas Booster (P1)	Increases the pressure of the gas mixture into the mixing vessel. Air operated single air head, single acting, and single stage booster.
Vacuum Pump (P2)	Evacuates the mixing vessel and equilibrium cell. Turbo molecular vacuum pump with backing diaphragm pump
Thermostat heating bath (T1)	Provides heat and maintains constant temperature in the heating jackets. Heating circulator with temperature controller.

Temperature of the cell is adjusted to the desired value by setting the temperature bath. 5mL of solvent is introduced to the equilibrium cell using metering pump. Pressure of the system is adjusted to the desired pressure. At this stage, the pressure of the mixing vessel is considered as the solvent vapor pressure, P_v Then, CO_2 will be transferred to mixing vessel to equilibrium cell. The number of moles of CO_2, n_{CO_2} transferred from mixing vessel to equilibrium cell is calculated using volume of vessel, temperature and pressure drop between mixing vessel and equilibrium cell.

$$n_{CO2} = \frac{V_T}{RT_a}\left(\frac{P_1}{z_1} - \frac{P_2}{z_2}\right) \quad \text{(Equation 7)}$$

Where;

$n_{CO2} = moles\ of\ carbon\ dioxide$
$V_T = Volume\ of\ gas\ container\ (mixing\ vessel)$
$T_a = Ambient\ temperature$
$P_1 = Pressure\ of\ mixing\ vessel$
$P_2 = Pressure\ of\ equilibrium\ cell$
$z_1 = Compressibility\ factor\ at\ P_1$
$z_2 = Compressibility\ factor\ at\ P_2$
$R = Ideal\ gas\ constant$

The compressibility factors are calculated using Peng Robinson equation of state (EOS). When thermodynamic equilibrium is achieved, the pressure of the equilibrium cell is recorded. The equilibrium pressure is calculation by using **Equation 8**.

$$P_{CO2} = P_T - P_V \quad \text{(Equation 8)}$$

Where;
$P_{CO2} = Equilibrium\ pressure$
$P_T = Total\ pressure$
$P_V = Vapor\ pressure\ of\ solutions$

The remaining moles of CO_2 gas in the equilibrium cell are calculated using **Equation 9**.

$$n_{CO_2}^{g} = \frac{V_g P_{CO_2}}{Z_{CO_2} RT} \quad \text{(Equation 9)}$$

Where;

$n_{CO_2}^{g} = moles\ of\ CO_2\ in\ gas\ phase$
$P_{CO2} = Equilibrium\ pressure$

$V_g = Over head\ gas\ volume$

$Z_{CO_2} = Compressibility\ factor\ of\ CO_2$

$T = Operating\ temperature$

$R = Ideal\ gas\ constant$

The moles of CO_2 are then calculated by using **Equation 10**.

$$n^l_{CO_2} = n_{CO_2} - n^g_{CO_2} \quad \text{(Equation 10)}$$

Where;

$n^l_{CO_2} = moles\ of\ CO_2\ in\ liquid\ phase$

$n^g_{CO_2} = moles\ of\ CO_2\ in\ gas\ phase$

$n_{CO2} = moles\ of\ CO_2$

The solubility is calculated as the ratio of mol CO_2 to mol of amine using **Equation 11**.

$$\alpha = \frac{n^l_{CO_2}}{n_{AM}} \quad \text{(Equation 11)}$$

Where;

$\alpha = solubility$

$n^l_{CO_2} = moles\ of\ CO_2\ in\ liquid\ phase$

$n_{AM} = moles\ of\ amine$

Mol of amine represents the moles of (PZ+BALA) in the liquid and calculated using the **Equation 12**.

$$n_{AM} = \frac{\rho V_l m_{(PZ+BALA)}}{M_{(PZ+BALA)}} \quad \text{(Equation 12)}$$

Where;

$n_{AM} = moles\ of\ amine$

$\rho = density\ of\ aqueoous\ solution$

$V_l = Liquid\ volume$

$m_{(\ PZ+BALA\ )} = mass\ fraction\ of\ (PZ + BALA)$

$M_{(\ PZ+BALA\ )} = Molecular\ weight\ of\ (PZ + BALA)$

The optimization on solubility is performed using the Response Surface Methodology (RSM). In order to investigate the influence of operating parameters on the CO_2 solubility, the total number of runs for the experiment is determined as 20. The operating parameters and its ranges of values are shown in **Table 4**. The low values are denoted as -1 while the high values are denoted as +1. These parameters are randomized to minimize the unexpected variability in the observed responses.

Table **4**: Operating parameters and its ranges of values

Parameters	-1	0	+1
A: B-alanine/Piperazine concentration	16%BALA-14%PZ	22%BALA-8%PZ	28%BALA-2%PZ
B: Pressure (bar)	1	5.6	10
C: Tempearture (^oC)	30	40	50

The formulation of a second order equation that describes the process. The general equation is as shown in **equation 13**.

$$B = b_o + b_1 X_1 + b_2 X_2 + b_3 X_3 + b_{11} X_1^2 + b_{22} X_2^2 + b_{33} X_3^2 + b_{12} X_1 X_2 + b_{13} X_1 X_3 + b_{23} X_2 X_3 \quad \text{(Equation 13)}$$

Here, B is the solubilty, b_o is the intercept term, b_1, b_2 b_3 and b_4 are linear coeffiecients, b_{11}, b_{22}, b_{33}, b_{44} are quadratic equations, b_{12}, b_{13}, b_{14}, b_{23}, b_{24}, b_{34} are interactive coefficients and X_1, X_2, X_3, X_4 are the independent variables.

3.5 Key Milestones

Problem Statement and Objective of the Project: Identifying the purpose of conduction the research work.

↓

Literature Review: Information gathering through journals and internet sources to obtain relevant literatures for the research project.

↓

Experiment Design: Identifying the subjects that need to be investigated, the experimental procedures, equipment and chemicals needed, as well as results collection.

↓

Data Analysis and Interpretation: The findings obtained are analyzed and interpreted critically using graphs and tables. Calculation will be performed. Comparison with other literature readings will also be done.

↓

Documentation and Reporting: The research work will be documented and reported in detail. Recommendations and future work expansion will also be discussed.

3.6 Gantt Chart

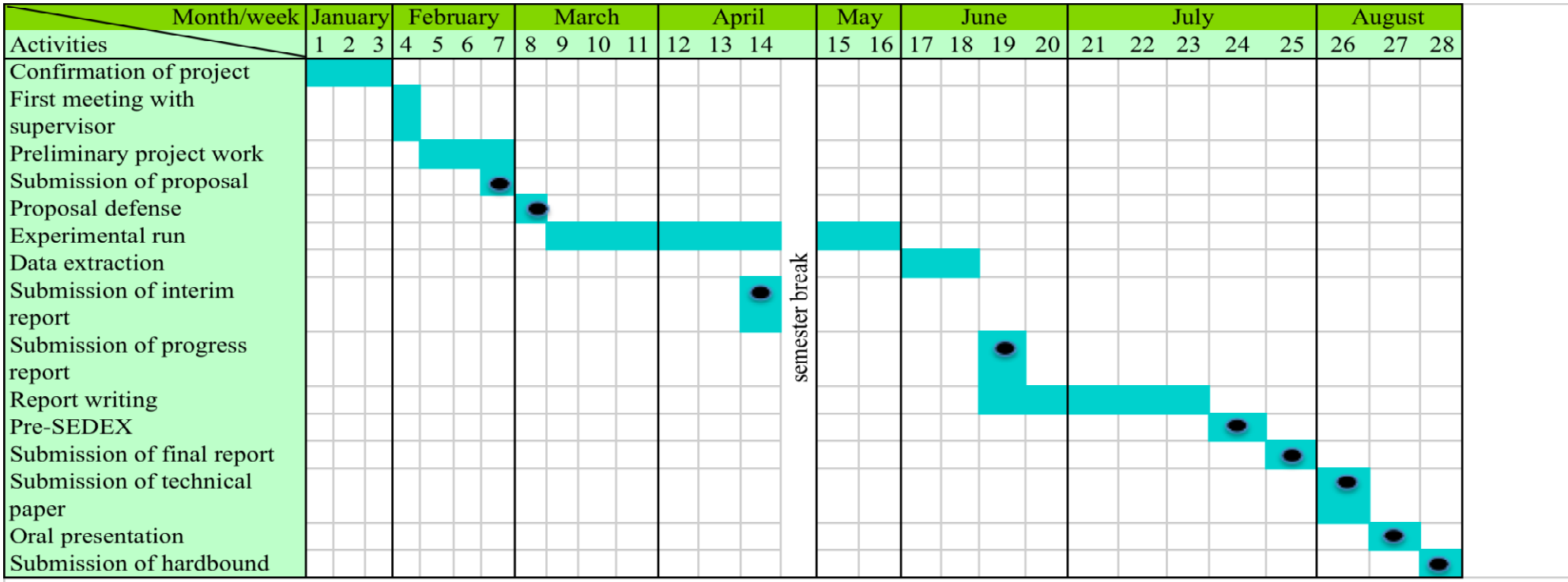

Key milestones are indicated in the black dotted symbol.

CHAPTER 4: RESULTS AND DISCUSSION

Physicochemical properties such as the density, viscosity, surface tension, refractive index and thermal decomposition of piperazine activated aqueous solution of B-alanine (BALA+PZ) were measured experimentally for three various concentrations of BALA and PZ over a wide range of temperature. The measured densities of piperazine activated aqueous solution of B-alanine (BALA+PZ) at temperature range from (30 to 60)^{o}C are shown in **Table 5**.

Table 5: Densities (ρ/ g.cm^{-3}) of piperazine activated aqueous solution of B-alanine from (30 to 60)^{o}C

Concentration (%BALA-%PZ)	**Temperature (^{o}C)**			
	30	40	50	60
16%BALA-14%PZ	1.05920	1.05479	1.05000	1.04481
22%BALA-8% PZ	1.07059	1.06593	1.06094	1.05497
28%BALA-2%PZ	1.09292	1.08863	1.08401	1.07909

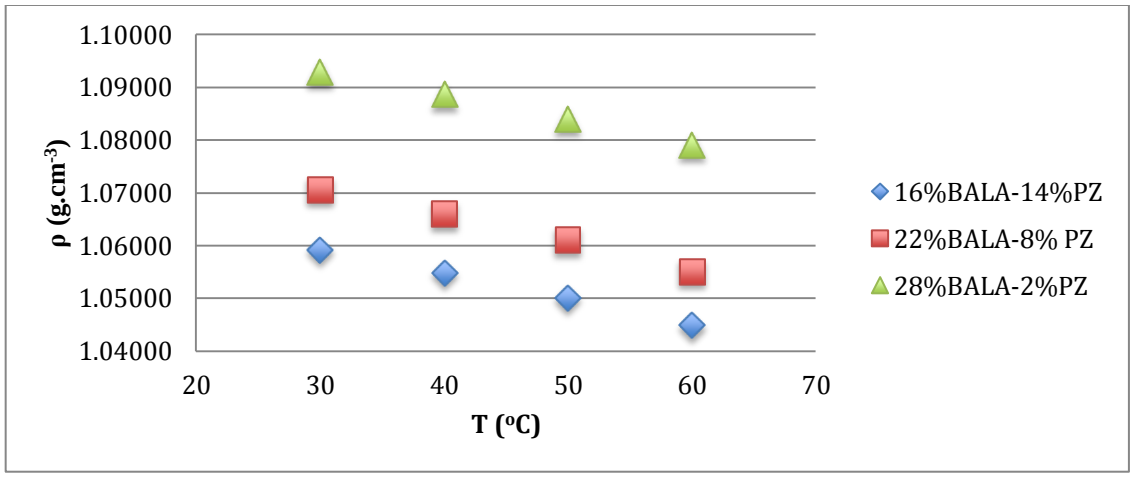

Figure 6: Plot of density,ρ of piperazine activated aqueous solution of B-alanine against temperature T from (30 to 60)^{o}C

The plot of density versus temperature is shown in **Figure 6**. From the plot, it can be seen that, as the mass percentage of B-alanine increases, the density is increased. However, with increasing temperature, the density of piperazine activated aqueous solution decreases. This is because, at higher temperature range, the spacing between

molecules is wider. The density trend of piperazine activated aqueous solution of B-alanine is similar to previous reported work that uses piperazine as promoter. The viscosity data of piperazine activated aqueous solution of B-alanine at temperature range of (30 to 60)^{o}C are listed in **Table 6**. The plot of viscosity versus temperature is shown in **Figure 7**.

Table 6: Viscosity (η /mPa.s of piperazine activated aqueous solution of B-alanine (30 to 60)^{o}C

Concentration (%BALA-%PZ)	**Temperature (^{o}C)**			
	30	40	50	60
16%BALA-14%PZ	3.2301	2.4888	1.9784	1.6131
22%BALA-8% PZ	2.6387	2.1288	1.7212	1.4233
28%BALA-2%PZ	2.2362	1.8020	1.5109	1.3091

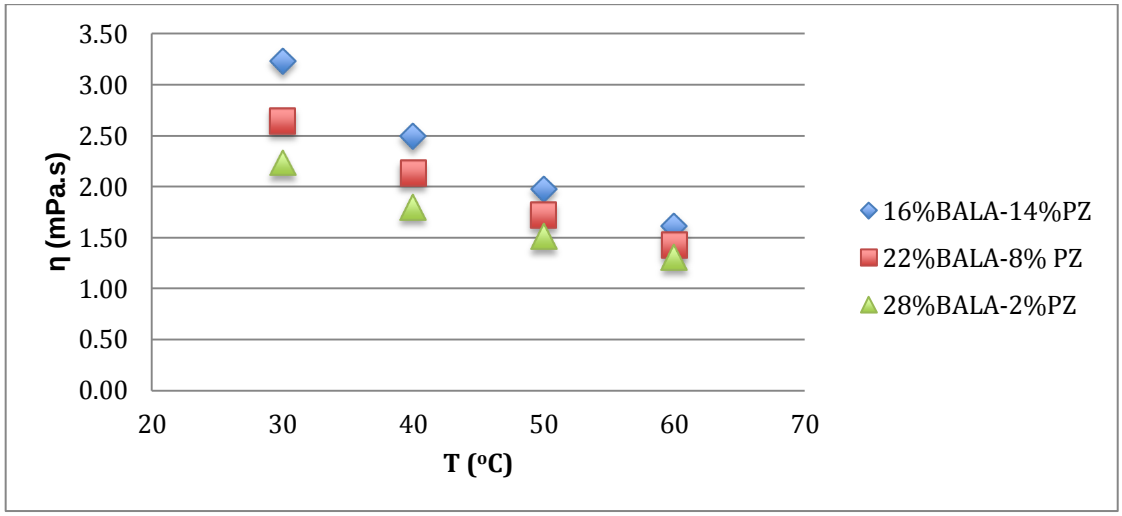

Figure 7: Plot of viscosity, η of piperazine activated aqueous solution of B-alanine against temperature T from (30 to 60)^{o}C

Analysis of the result shows that the viscosity decreases as the temperature increase. Reason being, the internal resistance of molecules decreases with the increase in temperature and directly allow the solution molecules to flow easily, thus reducing its viscosity. Besides that, the increase in mass percentage of piperazine will increase the viscosity of the solutions. High B-alanine mass percentage may lead to a rise in viscosity due to higher molecular resistance. The experimental data for refractive index of piperazine activated aqueous solution of B-alanine at temperature range of

(30 to 60)^{o}C are listed in **Table 7** and **Figure 8** shows its relationship versus temperature.

Table 7: Refractive index ($\mathbf{n_D}$) of piperazine aqueous solution of B-alanine from (30 to 60)^{o}C

Concentration (%BALA-%PZ)	**Temperature (K)**			
	30	40	50	60
16%BALA-14%PZ	1.387893	1.386774	1.385750	1.384730
22%BALA-8% PZ	1.387690	1.38637	1.385344	1.384380
28%BALA-2%PZ	1.387505	1.38624	1.385070	1.384000

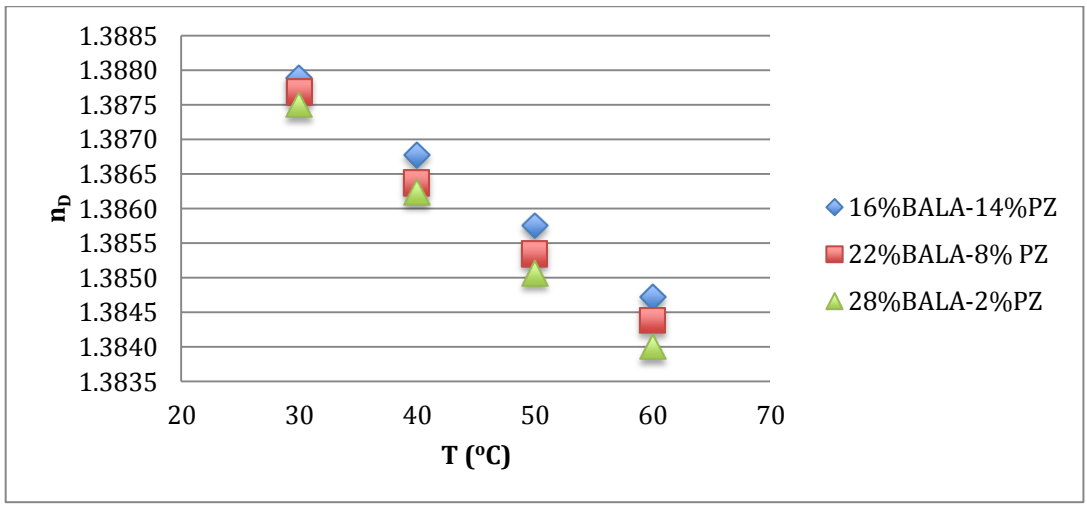

Figure 8: Plot of refractive index $\mathbf{n_D}$ of piperazine activated aqueous solution of B-alanine against temperature T from (30 to 60)^{o}C

From **Figure 8**, the refractive index increases with increasing piperazine concentration. Meanwhile, refractive index decreases slowly as the temperature increase. The increase in the speed of particle in piperazine activated aqueous solution of B-alanine caused fewer molecules strike by light and resulting in the reducing refractive index. The refractive index trend that decreases with increasing temperature is similar as reported in other literature that uses different solvents. The experimental data for surface tension of piperazine activated aqueous solution at temperature range of (30 to 60)^{o}C are consolidated in **Table 8** and **Figure 9** shows the plot of surface tension versus temperature.

Table 8: Surface tension (σ / mN.m^{-1}) of piperazine aqueous solution of B-alanine from (30 to 50)^{o}C

Concentration (%BALA-%PZ)	Temperature (^{o}C)		
	30	40	50
16%BALA-14%PZ	62.83	64.87	67.60
22%BALA-8% PZ	65.13	66.30	68.16
28%BALA-2%PZ	66.86	68.81	69.49

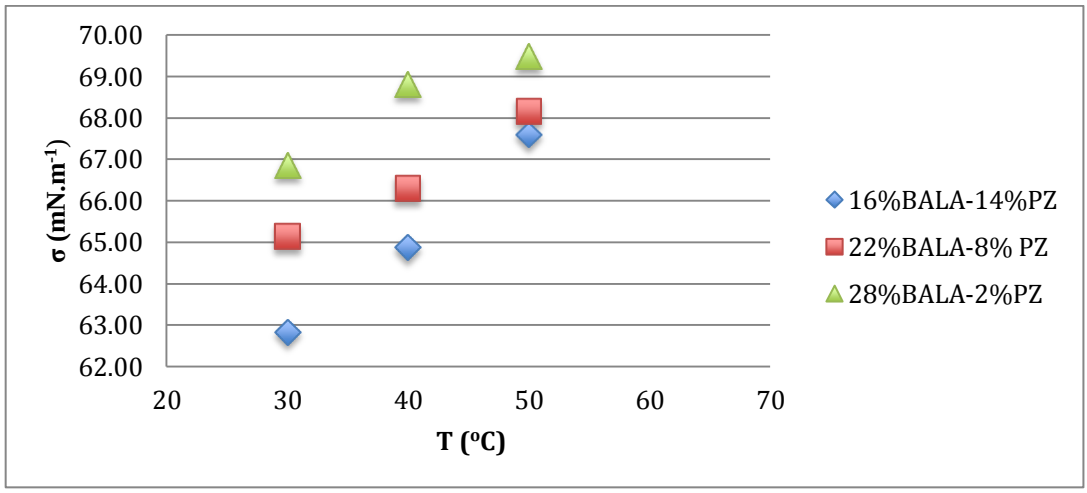

Figure 9: Plot of surface tension, σ of piperazine aqueous solution of B-alanine from (30 to 50)^{o}C

It was observed that, the surface tension increase when the percentage of B-alanine increases. Besides that, as the temperature increases, the surface tension will also increase.

The measured data of density, viscosity, refractive index and surface tension were correlated as a function of temperature using linear regression:

$$Y = A_0 + A_1(T/C) \qquad \text{(Equation 14)}$$

Where;

$Y = density, surface\ tension, refractive\ index\ or\ viscosity$

$A_o = Constants$

$A_1 = Fitting\ parameter$

$T = Temperature$

The least-squares method are used to calculate the fitting parameters and consolidated in **Table 9** with its respective standard deviations. Standard deviations are measured for all physicochemical properties by using the following equation:

$$SD = \left[\frac{\sum_i^n (X_{exp} - X_{calc})^2}{n}\right]^{0.5} \quad \text{(Equation 15)}$$

Where;

$SD = Standard\ deviations$

$X_{exp} = Experimental\ data$

$X_{calc} = Calculated\ data$

$n = number\ of\ experimental\ data\ points$

Table 9: Fitting parameters of Equation 14-15 to correlate physicochemical properties of piperazine activated aqueous solution of B-alanine

	Ao	**A_1**	**SD**
16%BALA-14%PZ			
Density (ρ/ g.cm^{-3})	1.0738	-0.0005	0.00009487
Viscosity (η /mPa.s)	4.7402	-0.0536	0.09449024
Refractive index (n_D)	1.3910	-0.0001	0.00022244
Surface tension (σ / mN.m^{-1})	55.56	0.2385	0.16263456
22%BALA-8% PZ			
Density (ρ/ g.cm^{-3})	1.0864	-0.0005	0.00088508
Viscosity (η /mPa.s)	3.8022	-0.0405	0.05303541
Refractive index (n_D)	1.3909	-0.0001	0.00047554
Surface tension (σ / mN.m^{-1})	60.47	0.1515	0.16263472
28%BALA-2%PZ			
Density (ρ/ g.cm^{-3})	1.1069	-0.0005	0.00182219
Viscosity (η /mPa.s)	3.0971	-0.0307	0.05842059
Refractive index (n_D)	1.3905	-0.0001	0.00035444
Surface tension (σ / mN.m^{-1})	63.127	0.1315	0.29934206

Calculated and measured physicochemical properties are shown in table and graph in the Appendix and are correlated in a linear relationship to each other.

The piperazine activated aqueous solution of B-alanine solubility towards CO_2 was measured with wide range of concentrations (16%BALA/14%PZ, 22%BALA/8%PZ, 28%BALA/2%PZ) at pressure range from 1bar to 10bar. The solubility was measured at three temperatures (30, 40 and 50) ^{0}C.

Table 10: Solubility of CO_2 in piperazine activated aqueous solution of B-alanine at temperature range of (30-60)^{0}C and pressure of (1-10)bar

Std	Run	Block	Factor 1	Factor 2	Factor 3	Response 1
			A: Concentration (wt%)	B:Temperature (^{o}C)	C:Pressure (bar)	Solubility (α)
1	1	Block 1	16%BALA-14%PZ	30.00	1.00	0.30
3	2	Block 1	16%BALA-14%PZ	30.00	10.00	2.58
9	3	Block 1	16%BALA-14%PZ	40.00	5.50	1.01
5	4	Block 1	16%BALA-14%PZ	50.00	1.00	0.23
7	5	Block 1	16%BALA-14%PZ	50.00	10.00	1.24
11	6	Block 1	22%BALA-8%PZ	40.00	1.00	0.23
15	7	Block 1	22%BALA-8%PZ	40.00	5.50	0.73
19	8	Block 1	22%BALA-8%PZ	40.00	5.50	0.73
17	9	Block 1	22%BALA-8%PZ	40.00	5.50	0.73
13	10	Block 1	22%BALA-8%PZ	40.00	5.50	0.73
16	11	Block 1	22%BALA-8%PZ	40.00	5.50	0.73
20	12	Block 1	22%BALA-8%PZ	40.00	5.50	0.73
18	13	Block 1	22%BALA-8%PZ	40.00	5.50	0.73
14	14	Block 1	22%BALA-8%PZ	50.00	5.50	0.58
2	15	Block 1	28%BALA-2%PZ	30.00	1.00	0.23
10	16	Block 1	28%BALA-2%PZ	40.00	5.50	0.67
6	17	Block 1	28%BALA-2%PZ	50.00	1.00	0.20
8	18	Block 1	28%BALA-2%PZ	50.00	10.00	1.25
4	19	Block 1	28%BALA-2%PZ	30.00	10.00	2.29
12	20	Block 1	22%BALA-8%PZ	40.00	10.00	1.27
6	19	Block 1	28%BALA-2%PZ	50.00	1.00	0.20

Table 10 presents the measured solubility data as a function of concentration, temperature and pressure. The results obtained in **Table 10** showed that the solubility ranged from 0.20 to 2.58 depending on the process parameters. ANOVA (analysis of variance) is then applied to further study the solubility effect based on process parameter concentration, temperature and pressure. The result of the analysis is the quadratic model as shown below:

$$\text{Solubility} = 3.37077 - 0.17195A + 0.31828B + 0.0069406C + 5.111364\text{E-}003A^2 + 7.60943\text{E-}003B^2 + 1.19091\text{E-}003C^2 - 4.67593\text{E-}003AB - 1.43750\text{E-}003AC - 2.91667\text{E-}003BC \quad \text{(Equation 16)}$$

The quadratic model represents solubility as the response, A as the coded value for B-alanine and piperazine concentration, B as the coded value for pressure, C as the coded value for temperature. The value of R^2 from the ANOVA analysis describes if the model fits the experimental data. The closer the value of R^2 to unity (value of 1), the better the fitting of the model with the experimental data obtained. It can be said that the predicted values match the observed values reasonably well within the ranges of operating parameters, with an R^2 value of 0.9563. The given equation is reliable and applicable in representing the solubility on piperazine activated aquesous solution on CO_2 solubility and can also be used to simulate the reaction.

The statistical ANOVA analysis for the quadratic model as shown in **Table 11**. The model F-value is 24.29 and it implies that the model is significant. 0.01% chance of that a "Model F-Value" this large occur due to noise.Parameter B (pressure) has the highest F-value which is 170.59 and it indicates the most influencing parameter for the solubility as compared to the other three parameters.

Table 11: ANOVA analysis of solubility

Source	Sum of Squares	DF	Mean Square	F Value	Prob > F
Model	8.64	9	0.96	24.29	<0.0001 significant
A	0.33	1	0.33	8.29	0.0164
B	6.74	1	6.74	170.58	< 0.0001
C	0.48	1	0.48	12.03	0.0060
A^2	0.093	1	0.093	2.36	0.1556
B^2	0.065	1	0.065	1.65	0.2276
C^2	0.039	1	0.039	0.99	0.3439
AB	0.13	1	0.13	3.23	0.1027
AC	0.060	1	0.060	1.51	0.2478
BC	0.14	1	0.14	3.49	0.0914
Residual	0.4	10	0.0040		
Lack of Fit	0.4	5	0.079		
Pure Error	0.000	5	0.000		

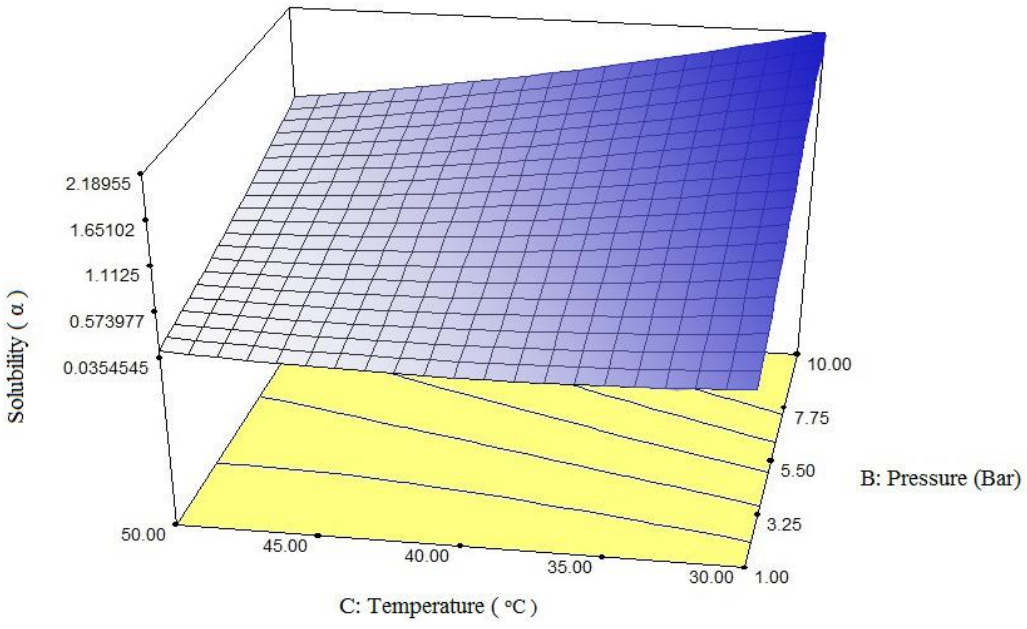

Figure 10: Plot of piperazine activated aqueous solution of B-alanine solubility towards CO_2 against pressure and temperature

Generally, the expected trend is solubility increases with decreasing temperature and increasing pressure. **Figure 10** is the representation of piperazine activated aqueous solution of B-alanine solubility as a function of pressure and temperature.

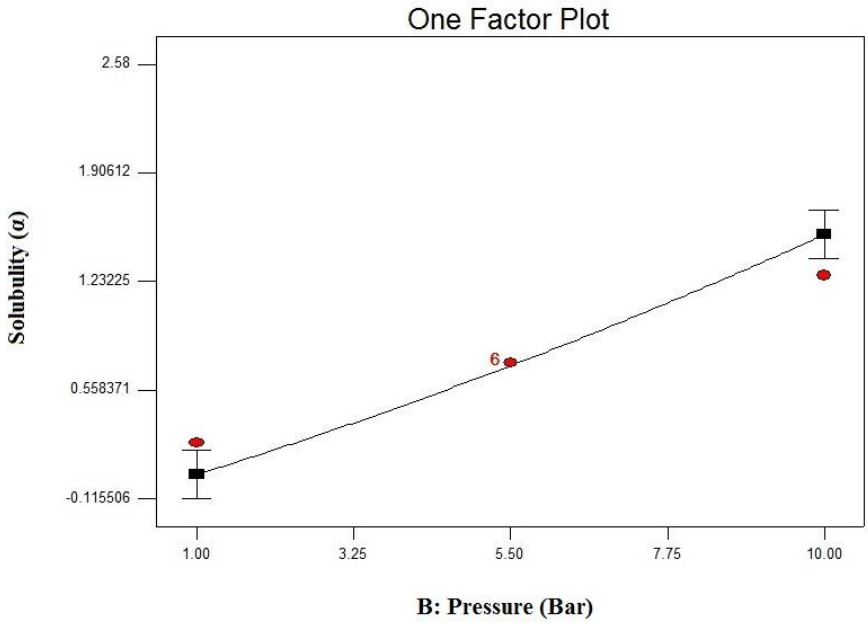

Figure 11: Plot of of piperazine activated aqueous solution of B-alanine solubility towards CO_2 against pressure from (1 to10) bar

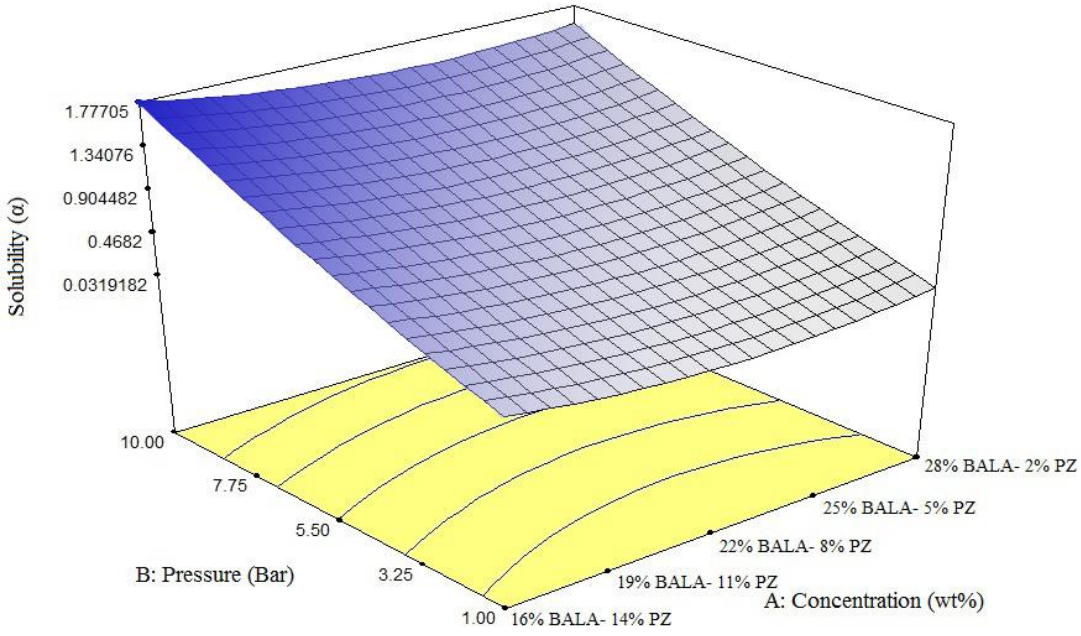

Figure 12: Plot of piperazine activated aqueous solution of B-alanine solubility towards CO_2 against pressure and concentration

Figure 11 and **Figure 12** shows that solubility of CO_2 increases with increasing pressure at any given solvent concentration. This observation shows that pressure has a positive effect on CO_2 loading.

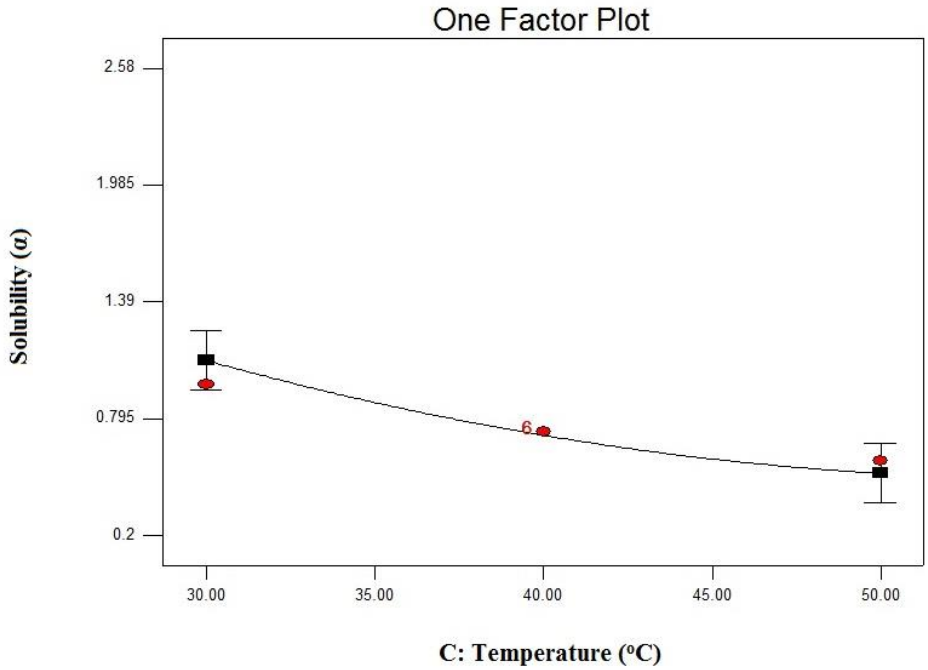

Figure 13: Plot of piperazine activated aqueous solution of B-alanine solubility towards CO_2 against temperature

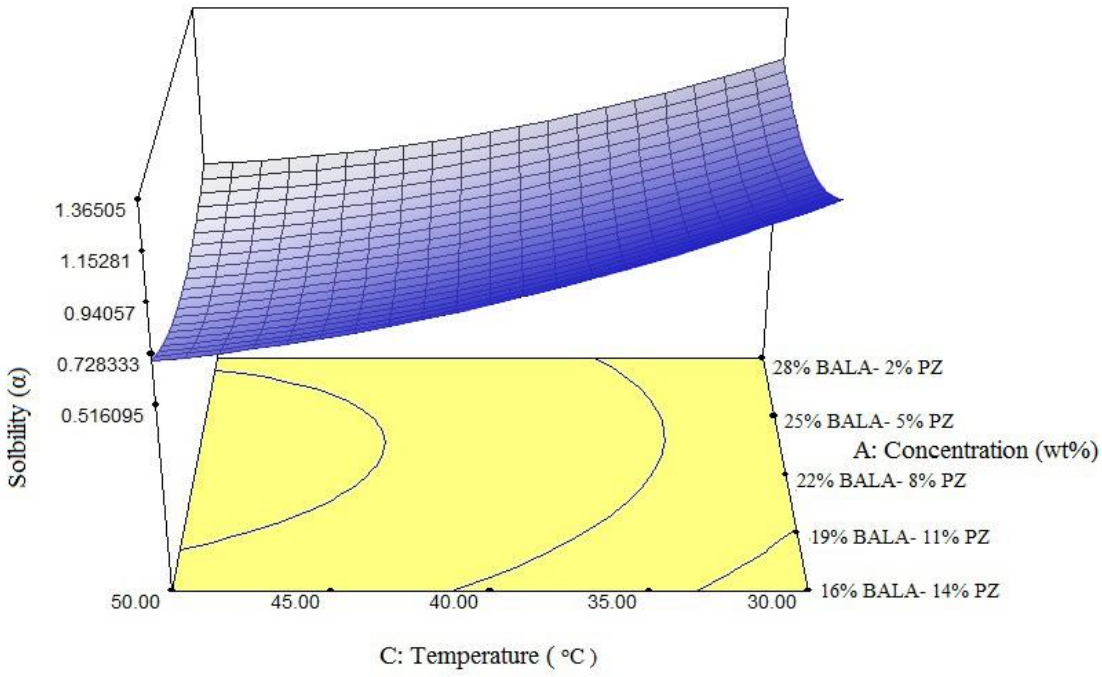

Figure 14: Plot of of piperazine activated aqueous solution of B-alanine solubility towards CO_2 temperature and concentration

Figure 13 and **Figure 14** show that at any given concentrations, CO_2 loading decreases when temperature increases. The negative effect of CO_2 loading at high temperature might due to high vapor pressure.

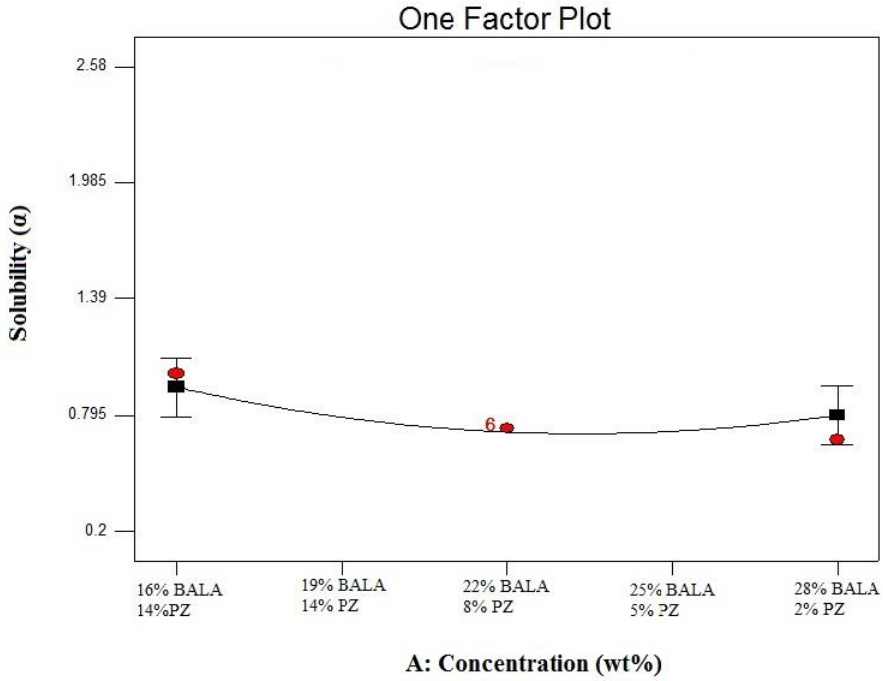

Figure 15: Plot of piperazine activated aqueous solution of B-alanine solubility towards CO_2 against B-alanine and piperazine concentrations

The effect of piperazine addition as promoter on the solubility can be seen **in Figure 12, 14** and **15. Figure 16** shows that increasing the piperazine concentration in the solvent will slowly increase the CO_2 loading of the respective solvent.

From the reported piperazine activated aqueous solution of B-alanine performance in this work, this solvent can be a potentially effective solvent that can be used as CO_2 removal from different gaseous streams and fit to be used by the industry.

CHAPTER 5: CONCLUSION

5.1 Conclusion

The physicochemical properties of piperazine activated aqueous solution of B-alanine which is density, viscosity, solubility and refractive index were measured at a wide range of temperature (30- 60) ^{0}C. Density, viscosity and refractive index tend to decreases with increasing pressure. Meanwhile, surface tension tends to increase with increasing temperature. Mathematical fitting equation of least square method was used to find correlation of experimental data in order to generate calculated data. The calculated standard deviations of experimental data are in good agreement with the calculated data. Solubility of CO_2 in piperazine activated aqueous solution of B-alanine was measured over a wide temperature and pressure range. The pressure are varied from 1 bar to 10 bar at three temperatures (30, 40, 50) ^{0}C. It can be conclude that solubility increases with decreasing temperature and increasing pressure. Higher piperazine concentration in B-alanine solutions will contribute to high CO_2 loading capacity. Piperazine activated aqueous solution of B-alanine can be a potential solvent to be used by the industry as an agent for CO_2 capture.

5.2 Future Work

The usage of different amino acids as solvent for CO_2 capture can be an alternative for alkanolamines. It is recommended that further study should be done on various amino acids that exhibit almost similar functional group as commercialized alkanolamines.

REFERENCES

Astarita, G., Savage, D. W., & Longo, J. M. (1981). Promotion of CO2 mass transfer in carbonate solutions. *Chemical Engineering Science, 36*(3), 581-588. doi: http://dx.doi.org/10.1016/0009-2509(81)80146-7

Bishnoi, S., & Rochelle, G. T. (2000). Absorption of carbon dioxide into aqueous piperazine: reaction kinetics, mass transfer and solubility. *Chemical Engineering Science, 55*(22), 5531-5543. doi: http://dx.doi.org/10.1016/S0009-2509(00)00182-2

Bougie, F., & Iliuta, M. C. (2011). CO2 Absorption in Aqueous Piperazine Solutions: Experimental Study and Modeling. *Journal of Chemical & Engineering Data, 56*(4), 1547-1554. doi: 10.1021/je1012247

Derks, P. W., Hogendoorn, K. J., & Versteeg, G. F. (2005). Solubility of N2O in and Density, Viscosity, and Surface Tension of Aqueous Piperazine Solutions. *Journal of Chemical & Engineering Data, 50*(6), 1947-1950. doi: 10.1021/je050202g

Geankoplis, C. J. (2003). *Transport Processes and Separation Process Principles: Includes Unit Operations*: Prentice Hall Professional Technical Reference.

Hook, R. J. (1997). An Investigation of Some Sterically Hindered Amines as Potential Carbon Dioxide Scrubbing Compounds. *Industrial & Engineering Chemistry Research, 36*(5), 1779-1790. doi: 10.1021/ie9605589

Mergler, Y., Gurp, R. R.-v., Brasser, P., Koning, M. d., & Goetheer, E. (2011). Solvents for CO2 capture. Structure-activity relationships combined with vapour-liquid-equilibrium measurements. *Energy Procedia, 4*(0), 259-266. doi: http://dx.doi.org/10.1016/j.egypro.2011.01.050

Muhammad, A., Mutalib, M. I. A., Wilfred, C. D., Murugesan, T., & Shafeeq, A. (2008). Viscosity, Refractive Index, Surface Tension, and Thermal Decomposition of Aqueous N-Methyldiethanolamine Solutions from (298.15 to 338.15) K. *Journal of Chemical & Engineering Data, 53*(9), 2226-2229. doi: 10.1021/je800282a

Rao, A. B., & Rubin, E. S. (2002). A Technical, Economic, and Environmental Assessment of Amine-Based CO2 Capture Technology for Power Plant

Greenhouse Gas Control. *Environmental Science & Technology*, *36*(20), 4467-4475. doi: 10.1021/es0158861

Sakwattanapong, R., Aroonwilas, A., & Veawab, A. (2005). Behavior of Reboiler Heat Duty for CO2 Capture Plants Using Regenerable Single and Blended Alkanolamines. *Industrial & Engineering Chemistry Research*, *44*(12), 4465-4473. doi: 10.1021/ie050063w

Shaikh, M. S., Shariff, A. M., Bustam, M. A., & Murshid, G. (2013). Physical Properties of Aqueous Blends of Sodium Glycinate (SG) and Piperazine (PZ) as a Solvent for CO2 Capture. *Journal of Chemical & Engineering Data*, *58*(3), 634-638. doi: 10.1021/je301091z

Shariff, A. M., Murshid, G., Lau, K. K., Bustam, M. A., & Ahamd, F. (2011). Solubility of CO2 in Aqueous Solution of 2-Amino-2-Methyl-1-Propanol at High Pressure. *60*.

Song, H.-J., Park, S., Kim, H., Gaur, A., Park, J.-W., & Lee, S.-J. (2012). Carbon dioxide absorption characteristics of aqueous amino acid salt solutions. *International Journal of Greenhouse Gas Control*, *11*(0), 64-72. doi: http://dx.doi.org/10.1016/j.ijggc.2012.07.019

Soosaiprakasam, I. R., & Veawab, A. (2008). Corrosion and polarization behavior of carbon steel in MEA-based CO2 capture process. *International Journal of Greenhouse Gas Control*, *2*(4), 553-562. doi: http://dx.doi.org/10.1016/j.ijggc.2008.02.009

Supap, T., Idem, R., Tontiwachwuthikul, P., & Saiwan, C. (2009). Kinetics of sulfur dioxide- and oxygen-induced degradation of aqueous monoethanolamine solution during CO2 absorption from power plant flue gas streams. *International Journal of Greenhouse Gas Control*, *3*(2), 133-142. doi: http://dx.doi.org/10.1016/j.ijggc.2008.06.009

APPENDICES

Calculated and measured data for physicochemical properties

Table 12: Calculated and measured value for density of (16%BALA-14%PZ)

Density ($g.cm^{-3}$)	Temperature (^oC)			
	30	40	50	60
Calculated (16%BALA-14%PZ)	1.0588	1.0538	1.0488	1.0438
Measured (16%BALA-14%PZ)	1.0592	1.0548	1.0500	1.0448

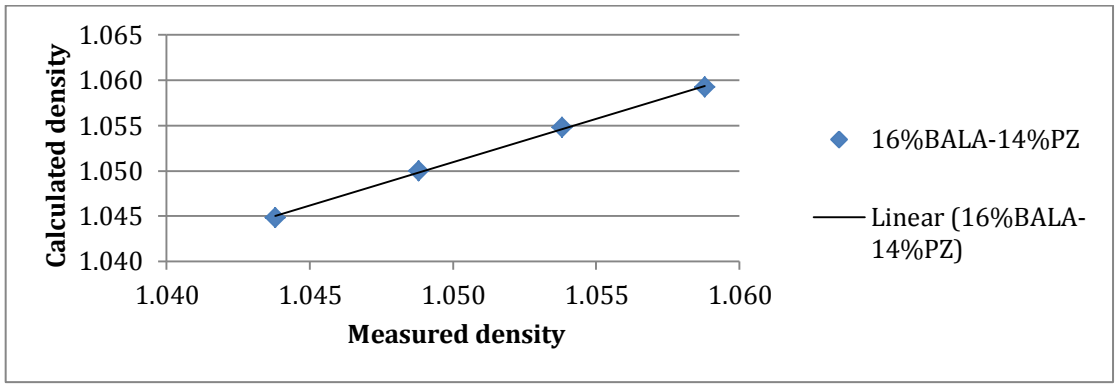

Figure 16: Calculated density vs. measured density of (16%BALA-14%PZ)

Table 13: Calculated and measured value for density of (22%BALA-8%PZ)

Density ($g.cm^{-3}$)	Temperature (^oC)			
	30	40	50	60
Calculated (22%BALA-8% PZ)	1.0714	1.0664	1.0614	1.0564
Measured (22%BALA-8% PZ)	1.0706	1.0659	1.0609	1.0550

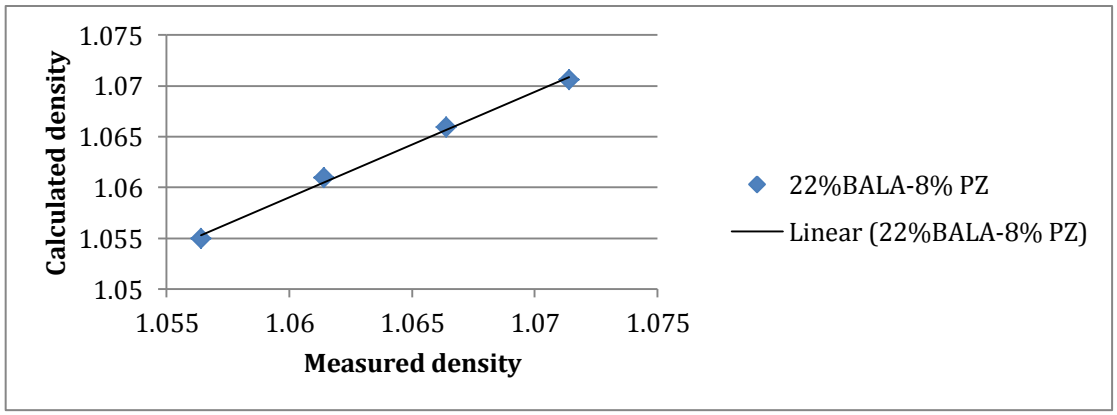

Figure 17: Calculated density vs. measured density of (22%BALA-8%PZ)

Table 14: Calculated and measured value for density of (28%BALA-2%PZ)

Density (g.cm^{-3})	Temperature (^{o}C)			
	30	40	50	60
Calculated (28%BALA-2%PZ)		1.0869	1.0819	1.0769
Measured (28%BALA-2%PZ)	1.0929	1.0886	1.0840	1.0791

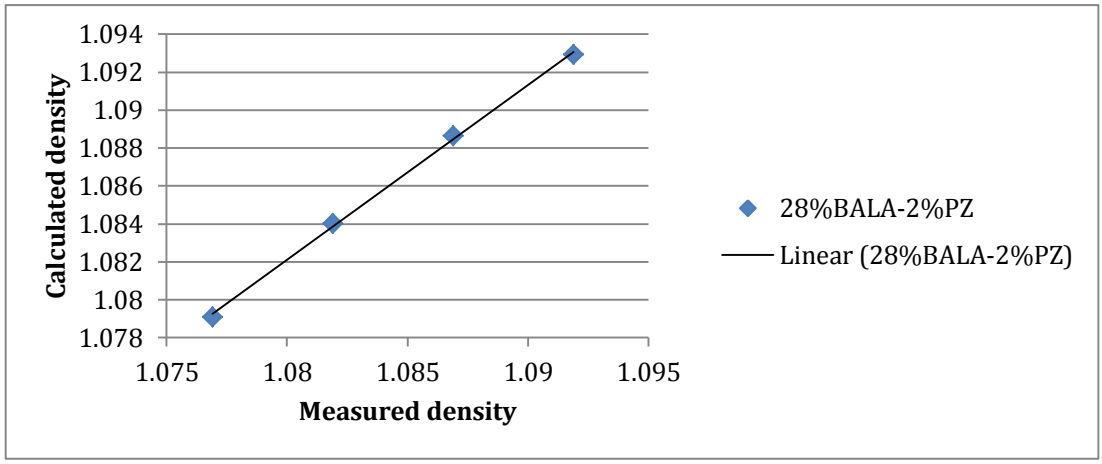

Figure 18: Calculated density vs. measured density of (28%BALA-2%PZ)

Table 15: Calculated and measured value for viscosity of (16%BALA-14%PZ)

Viscosity (mPa.s)	Temperature (^{o}C)			
	30	40	50	60
Calculated (16%BALA-14%PZ)	3.1322	2.5962	2.0602	1.5242
Measured (16%BALA-14%PZ)	3.2301	2.4888	1.9784	1.6131

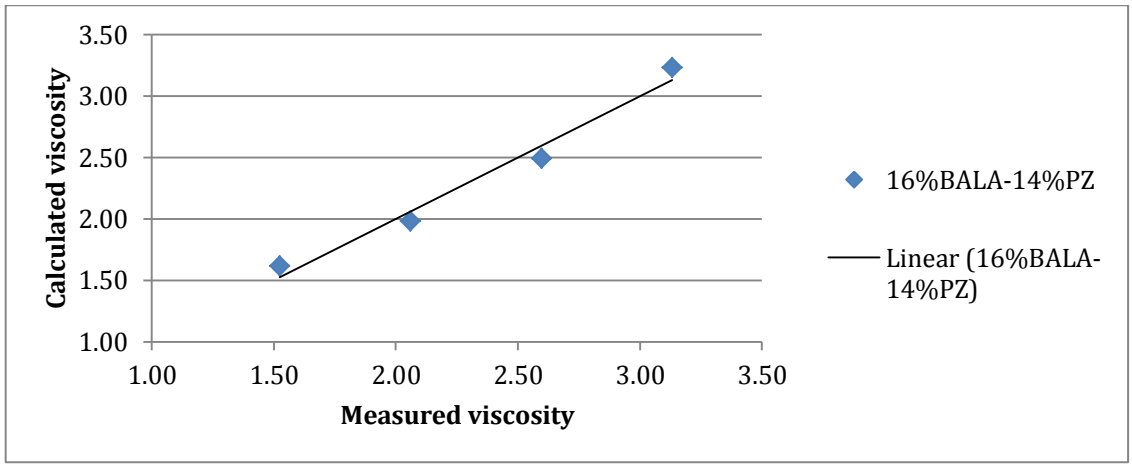

Figure 19: Calculated viscosity vs. measured viscosity of (16%BALA-14%PZ)

Table 16: Calculated and measured value for viscosity of (22%BALA-8%PZ)

Viscosity (mPa.s)	Temperature (^{o}C)			
	30	40	50	60
Calculated (22%BALA-8% PZ)	2.5872	2.1822	1.7772	1.3722
Measured (22%BALA-8% PZ)	2.6387	2.1288	1.7212	1.4233

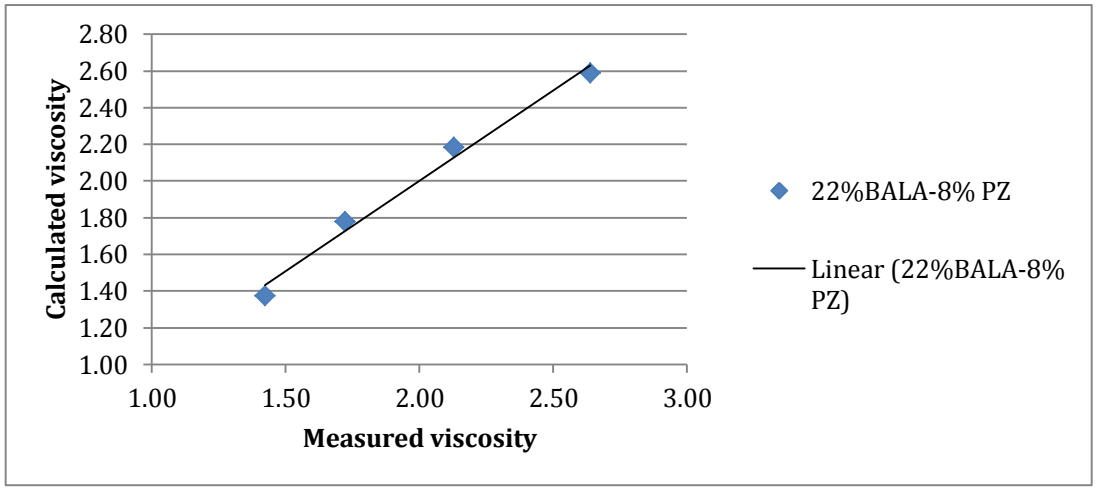

Figure 20: Calculated viscosity vs. measured viscosity of (22%BALA-8%PZ)

Table 17: Calculated and measured value for viscosity of (28%BALA-2%PZ)

Viscosity (mPa.s)	Temperature (^{o}C)			
	30	40	50	60
Calculated (28%BALA-2%PZ)	2.1761	1.8691	1.5621	1.2551
Measured (28%BALA-2%PZ)	2.2362	1.802	1.5109	1.3091

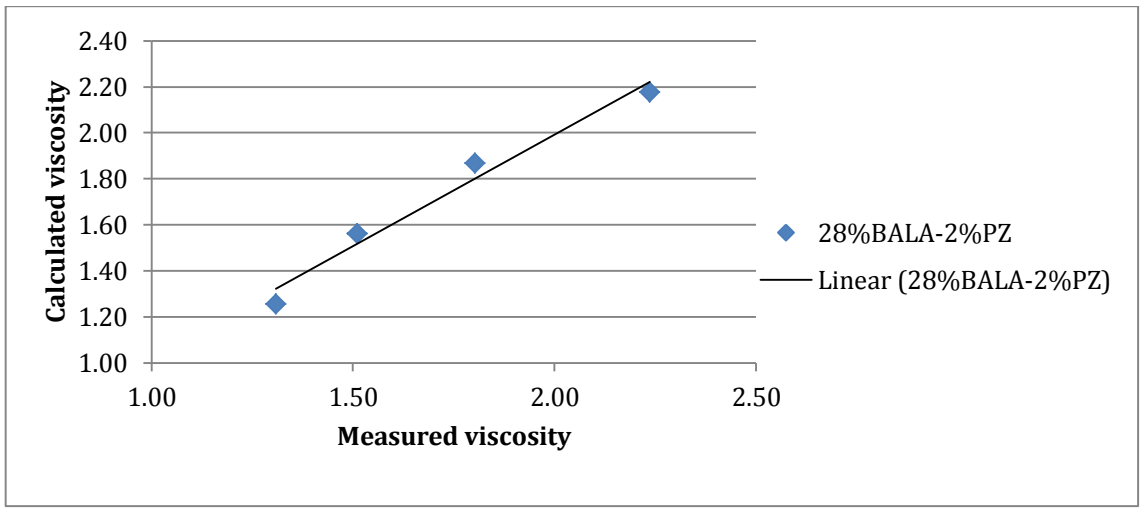

Figure 21: Calculated viscosity vs. measured viscosity of (28%BALA-2%PZ)

Table 18: Calculated and measured value for refractive index of (16%BALA-14%PZ)

Refractive Index (n_D)	Temperature (°C)			
	30	40	50	60
Calculated (16%BALA-14%PZ)	1.388	1.387	1.386	1.385
Measured (16%BALA-14%PZ)	1.388	1.387	1.386	1.385

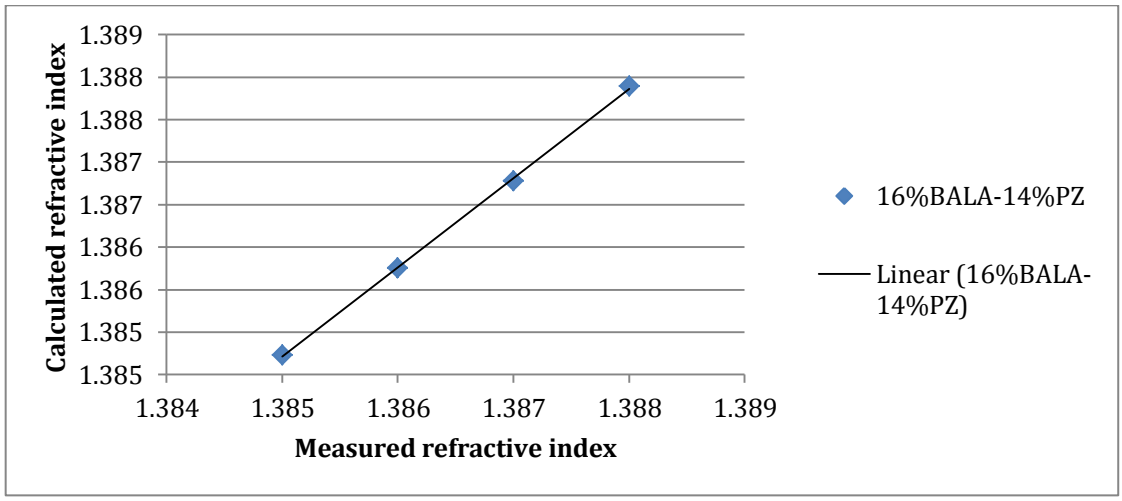

Figure 22: Calculated refractive index vs. measured refractive index of (16%BALA-14%PZ)

Table 19: Calculated and measured value for refractive index of (22%BALA-8%PZ)

Refractive Index (n_D)	Temperature (°C)			
	30	40	50	60
Calculated (22%BALA-8% PZ)	1.3879	1.3869	1.3859	1.3849
Measured (22%BALA-8% PZ)	1.3877	1.3864	1.3853	1.3844

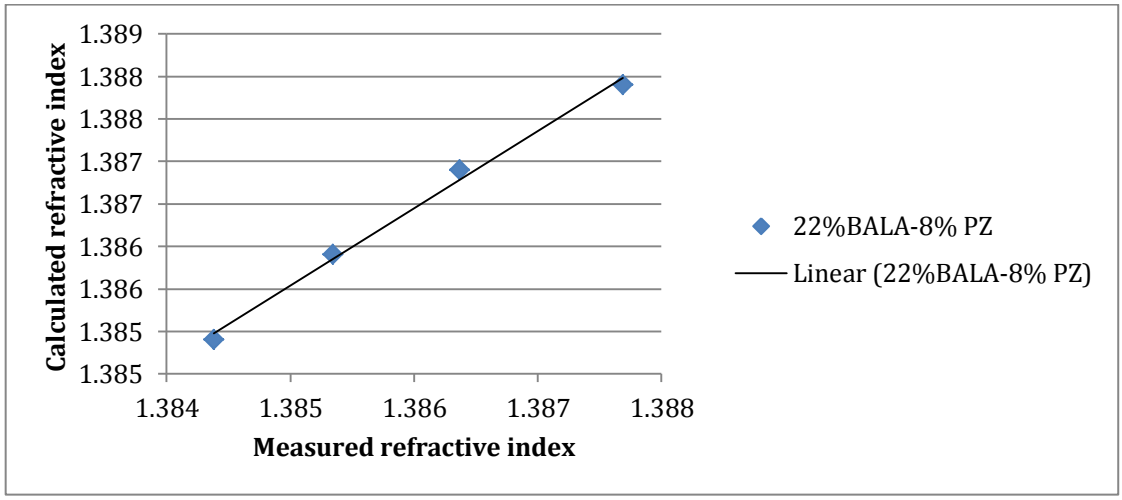

Figure 23: Calculated refractive index vs. measured refractive index of (22%BALA-8%PZ)

Table 20: Calculated and measured value for refractive index of (28%BALA-2%PZ)

Refractive Index (n_D)	Temperature (°C)			
	30	40	50	60
Calculated (28%BALA-2%PZ)	1.3875	1.3865	1.3855	1.3845
Measured (28%BALA-2%PZ)	1.3875	1.3862	1.3851	1.3840

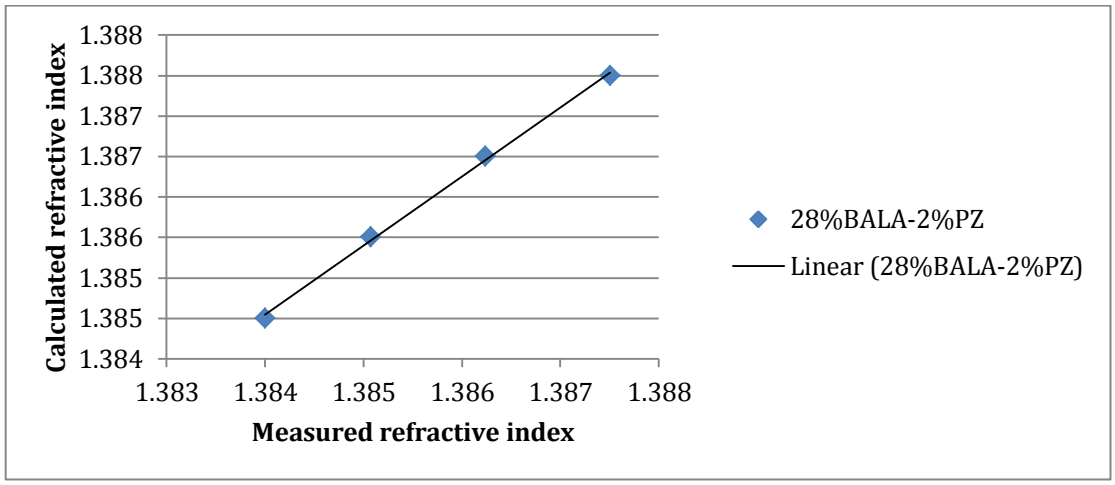

Figure 24: Calculated refractive index vs. measured refractive index of (28%BALA-2%PZ)

Table 21: Calculated and measured value for surface tension of (16%BALA-14%PZ)

Surface Tension ($mN.m^{-1}$)	Temperature (°C)		
	30	40	50
Calculated (16%BALA-14%PZ)	62.72	65.10	67.49
Measured (16%BALA-14%PZ)	62.83	64.87	67.60

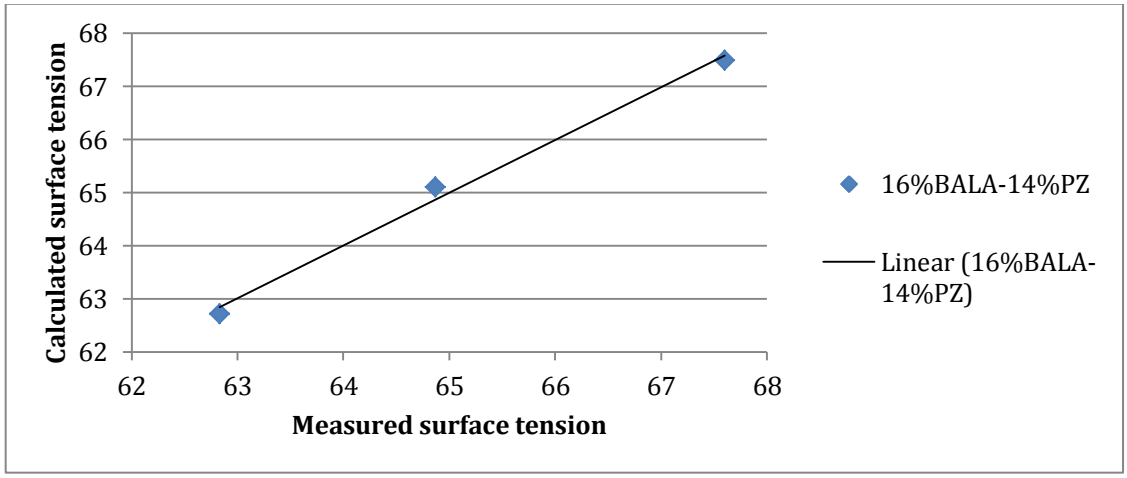

Figure 25: Calculated surface tension vs. measured surface tension of (16%BALA-14%PZ)

Table 22: Calculated and measured value for surface tension of (22%BALA-8%PZ)

Surface Tension ($mN.m^{-1}$)	Temperature (^oC)		
	30	40	50
Calculated (22%BALA-8% PZ)	65.015	66.53	68.045
Measured (22%BALA-8% PZ)	65.13	66.30	68.16

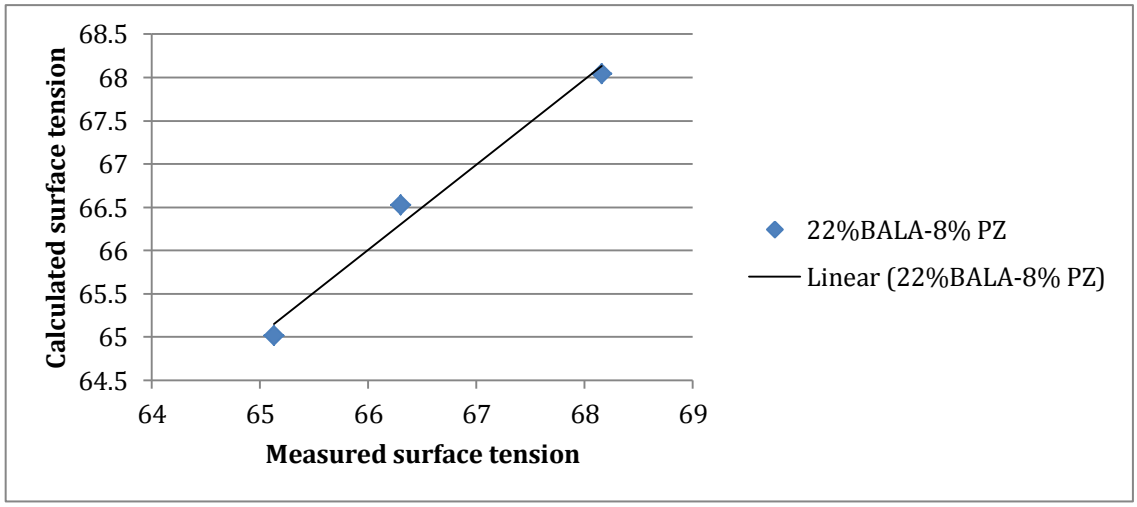

Figure 26: Calculated surface tension vs. surface tension of (22%BALA-8%PZ)

Table 23: Calculated and measured value for surface tension of (28%BALA-2%PZ)

Surface Tension ($mN.m^{-1}$)	Temperature (^oC)		
	30	40	50
Calculated (28%BALA-2%PZ)	67.07	68.39	69.70
Measured (28%BALA-2%PZ)	66.86	68.81	69.49

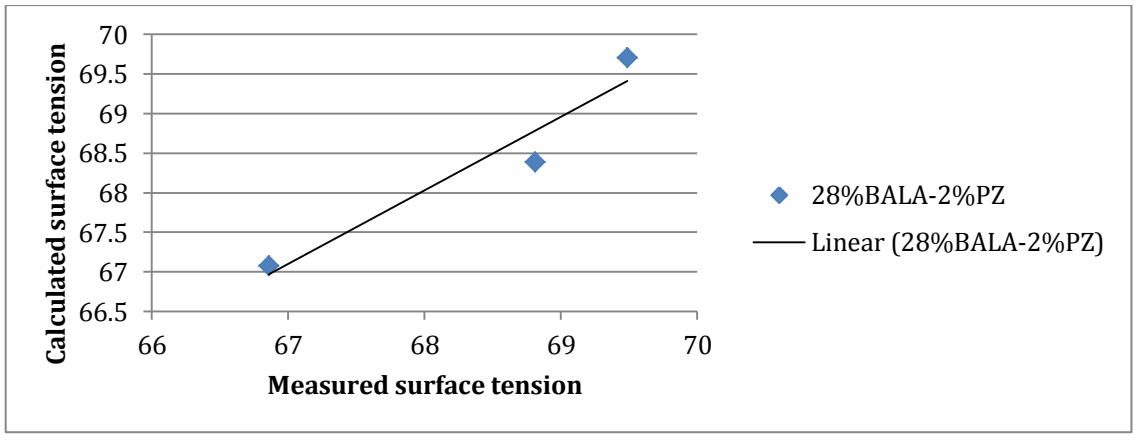

Figure 27: Calculated surface tension vs. measured surface tension of (28%BALA-2%PZ)

Surface tension experimental result

16% BALA- 14% PZ

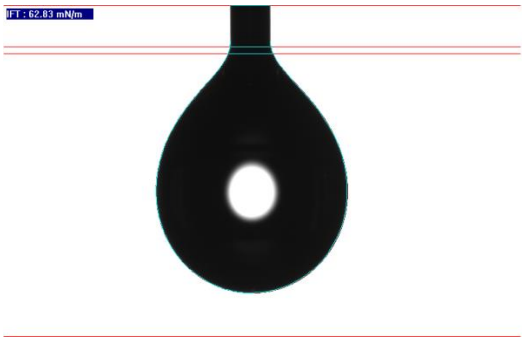

Figure 28: Surface tension of (16% BALA- 14% PZ) at 30^{o}C

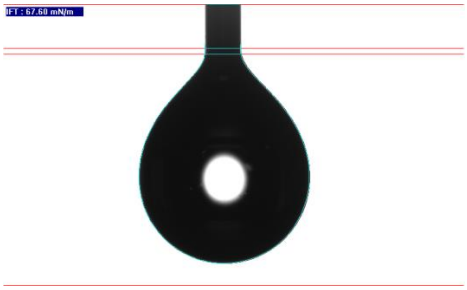

Figure 29: Surface tension of (16% BALA- 14% PZ) at 40^{o}C

Figure 30: Surface tension of (16% BALA- 14% PZ) at 50^{o}C

22% BALA- 8% PZ

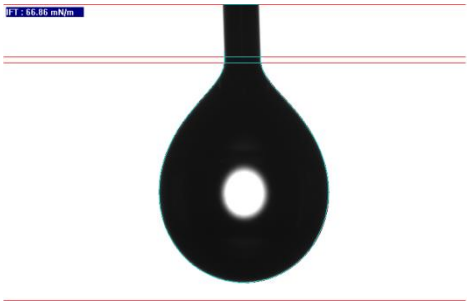

Figure 31: Surface tension of (22% BALA- 8% PZ) at 30^{o}C

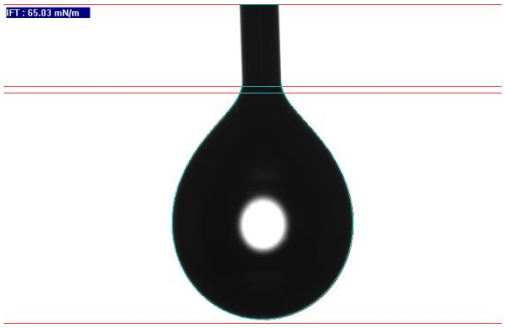

Figure 32: Surface tension of (22% BALA- 8% PZ) at 40^{o}C

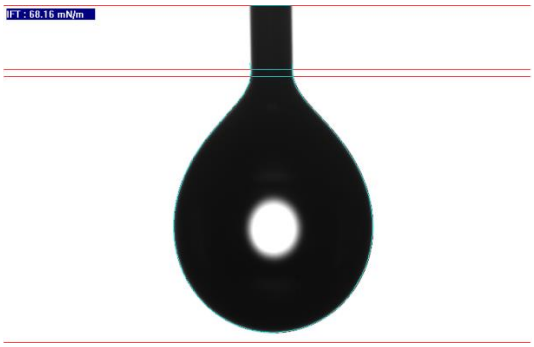

Figure 33: Surface tension of (22% BALA- 8% PZ) at 50^{o}C

28% BALA- 2% PZ

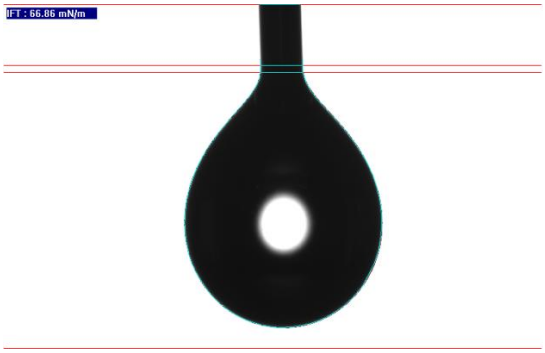

Figure 34: Surface tension of (28% BALA- 2% PZ) at 30^{o}C

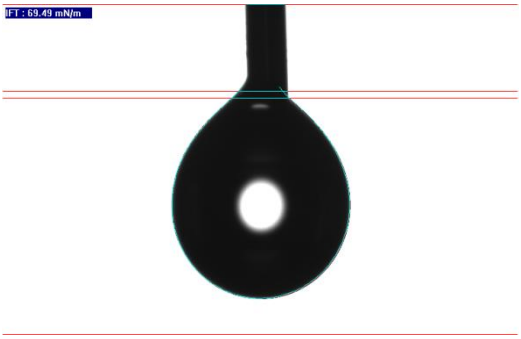

Figure 35: Surface tension of (28% BALA- 2% PZ) at 40^{o}C

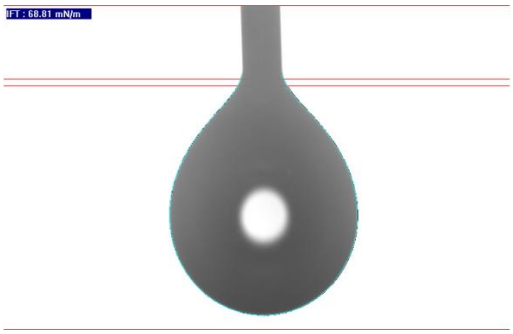

Figure 36: Surface tension of (28% BALA- 2% PZ) at 50^{o}C